

# Improved analytical solution for slip and interfacial stress in composite steel-concrete beam bonded with an adhesive

Bensatallah Tayeb<sup>a</sup> and Tahar Hassaine Daouadji\*

Laboratory of Geomatics and Sustainable Development, University of Tiaret, Algeria

(Received March 24, 2020, Revised May 27, 2020, Accepted May 30, 2020)

**Abstract.** In this paper, an improved theoretical interfacial stress and slip analysis is presented for simply supported composite steel-concrete beam bonded with an adhesive. The adherend shear deformations have been included in the present theoretical analyses by assuming a linear shear stress through the thickness of the adherends, while all existing solutions neglect this effect. Remarkable effect of shear deformations of elements has been noted in the results. It is observed that large shear is concentrated and slip at the edges of the composite steel-concrete. Comparing with some experimental results from references, analytical advantage of this improvement is possible to determine the normal and shear stress to estimate exact prediction of normal and shear stress interfacial along span between concrete and steel beam. The exact prediction of these stresses will be very important to make an accurate analysis of the mode of fracture. It is shown that both the normal and shear stresses at the interface are influenced by the material and geometry parameters of the composite steel-concrete beam. This research is helpful for the understanding on mechanical behavior of the connection and design of such structures.

**Keywords:** analytical solution; adhesive; shear deformations; slip; composite beam; interfacial stress

## 1. Introduction

The steel-concrete composite structures, which combine the high tensile strength of steel and the high compressive strength of concrete, have been widely used in multi-storey buildings and bridges all over the world. At the beginning of the 1960s, an efficient adhesive bonding technique (Henriques *et al.* 2020, Dezi *et al.* 1993, Adim *et al.* 2016c, Partov and Kantchev 2007, Tounsi *et al.* 2008, Jones *et al.* 1988, Krour *et al.* 2014, Liu *et al.* 2019, Panjehpour *et al.* 2016, Wang *et al.* 2020, Daouadji *et al.* 2016c, Lowe *et al.* 2020, Chen *et al.* 2019, Abderezak *et al.* 2018b, Benferhat *et al.* 2016c, Kumar *et al.* 2017, Larbi *et al.* 2007, Draiche *et al.* 2019, Draoui *et al.* 2019, Abderezak *et al.* 2019, Kaddari *et al.* 2020, Karami *et al.* 2019a, b, Adim *et al.* 2016d, Daouadji 2013, Mahmoudi *et al.* 2019, Medani *et al.* 2019, Adim and Daouadji 2016, Benferhat *et al.* 2016a, Benhenni *et al.* 2019a, Bensattalah *et al.* 2018, Rahmani *et al.* 2020, Daouadji *et al.* 2016a, Smith and Teng 2002, Tsai *et al.* 1998 and Zhao and Li 2008) was introduced to connect the concrete slab and the steel girder by an adhesive joint, not by the conventional metallic shear connectors. This so-called adhesive bonded steel-concrete composite beam is considered to be a very prospective alternate structure because it has the

---

\*Corresponding author, Professor, E-mail: daouadjitahar@gmail.com

<sup>a</sup> Ph.D., E-mail: tahar.daouadji@univ-tiaret.dz

advantages of relieving stress concentration, avoiding site welding, and using the prefabricated concrete slab. Recently, a number of studies on the experimental tests and numerical simulation of adhesive bonded steel-concrete composite beams have been presented in literatures (Bouazaoui *et al.* 2007, Lowe *et al.* 2020, Refrafi *et al.* 2020, Sahla *et al.* 2019, Tounsi *et al.* 2020, Zarga *et al.* 2019, Dezi *et al.* 1996, Gupta *et al.* 2015, Tahar *et al.* 2019, Lacki *et al.* 2019, Souici *et al.* 2013, Daouadji 2017, Benachour *et al.* 2008, Bouakaz *et al.* 2014, Chaded *et al.* 2018, Addou *et al.* 2019, Abualnour *et al.* 2019, Benferhat *et al.* 2016b, Rabia *et al.* 2019, Rabia *et al.* 2018, Benhenni *et al.* 2018, Alimirzaei *et al.* 2019, Benferhat *et al.* 2016b, Daouadji *et al.* 2008, Balubaid *et al.* 2019, Daouadji *et al.* 2016d, Belbachir *et al.* 2019, Belbachir *et al.* 2020, Berghouti *et al.* 2019, Abdederak *et al.* 2018a, Abdelhak *et al.* 2016, Belkacem *et al.* 2018, Adim *et al.* 2016a, Boukhelif *et al.* 2019, Bensattallah *et al.* 2016, Hadj *et al.* 2019, Adim *et al.* 2016b, Boulefrakh *et al.* 2019, Bousahla *et al.* 2020, Daouadji *et al.* 2016b, Boussoula *et al.* 2020, Daouadji and Benferhat 2016a, Boutaleb *et al.* 2019, Benhenni *et al.* 2019b, Rabahi *et al.* 2016, Chaabane *et al.* 2019, Henriques *et al.* 2020, Daouadji and Adim 2016c, Guenaneche and Tounsi 2014, Daouadji 2016c, Wang *et al.* 2020, Si and Au 2011).

The main objective of this research is to develop theoretical interfacial stress and slip are presented for simply supported composite steel-concrete beam. The adherent shear deformations have been included in the present theoretical analyses by assuming a linear shear stress through the thickness of the adherents. Hence, the adopted improved model describes better actual response of the composite steel-concrete beams and permits the evaluation of the interfacial stresses, the knowledge of which is very important in the design of such structures.

## 2. The method of solution

### 2.1 Assumptions of the present solution

This analysis takes into account the transverse shear stress and deformation in the steel beam and the reinforced concrete slab, but ignores the normal transverse stress therein. One of the analytical approaches for concrete slabs glued to steel beams (Fig. 1) was presented in order to compare it with an experimental analysis from the literature. This analytical approach is based on the following assumptions:

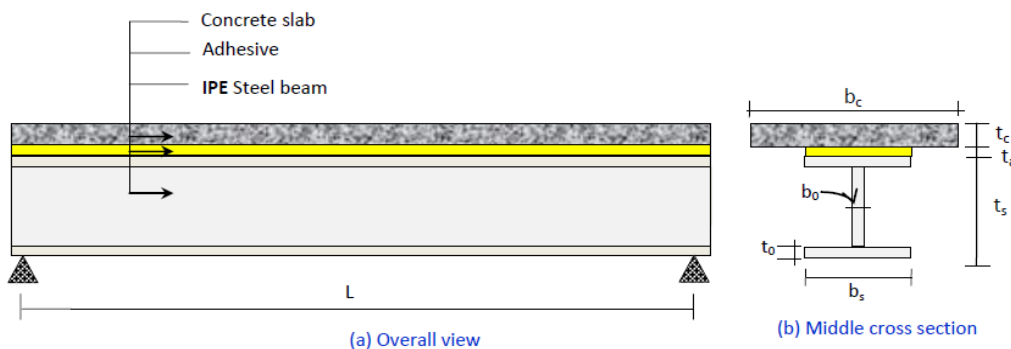


Fig. 1 Simply supported composite steel-concrete beam

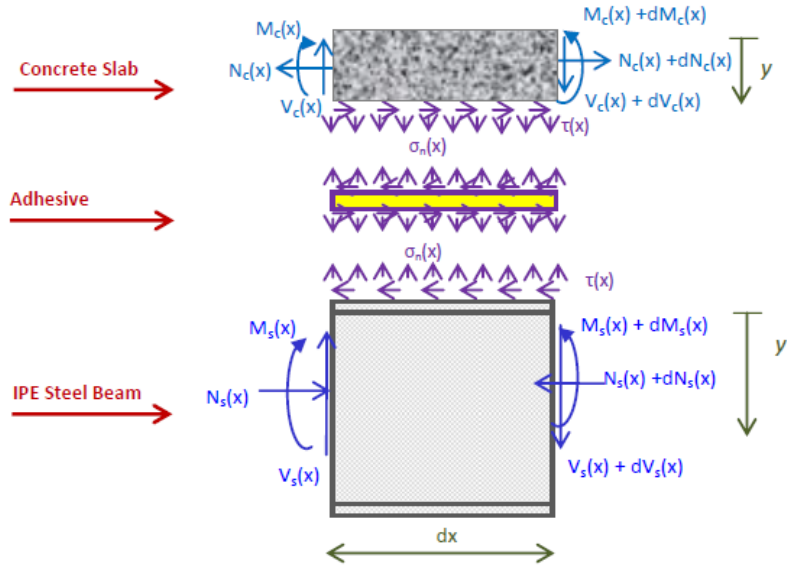


Fig. 2 Forces in infinitesimal element of a composite steel-concrete beam

- Elastic stress strain relationship for concrete, steel and adhesive;
- There is a perfect bond between the imperfect concrete slab and the steel beam;
- The adhesive is assumed to only play a role in transferring the stresses from the concrete slab to the steel beam;
- The stresses in the adhesive layer do not change through the direction of the thickness.

A differential section  $dx$ , can be cut out from the composite steel-concrete beam (Fig. 1) as shown in Fig. 2. The composite beam is made from three materials: concrete, adhesive and steel beam. In the present analysis, linear elastic behavior is regarded to be for all the materials; concrete and steel which must share in resisting the forces and moments caused by the transverse loads  $P$ . In the general case, the deformations that result must accommodate any interface slip in addition to the usual flexural and axial strains.

### 2.2 Shear stress distribution along the steel-concrete interface

The strains in the concrete near the adhesive interface and the external steel beam can be expressed as, respectively

$$\epsilon_c(x) = \frac{du_c(x)}{dx} = \epsilon_c^{(M)} + \epsilon_c^{(N)} \quad (1)$$

$$\epsilon_s(x) = \frac{du_s(x)}{dx} = \epsilon_s^{(M)} + \epsilon_s^{(N)} \quad (2)$$

Where  $u_c(x)$  and  $u_s(x)$  are the longitudinal displacements at the bottom of the concrete slab and the top of steel beam, respectively.  $\epsilon_c^{(M)}$  and  $\epsilon_s^{(M)}$  are the strains induced by the bending

moment at the concrete slab and beam steel, respectively and they are written as follow

$$\varepsilon_c^{(M)}(x) = \frac{du_c^{(M)}(x)}{dx} = \frac{y_c}{E_c I_c} M_c(x) \quad (3)$$

$$\varepsilon_s^{(M)}(x) = \frac{du_s^{(M)}(x)}{dx} = \frac{y_s}{E_s I_s} M_s(x) \quad (4)$$

Where  $E$  is the elastic modulus and  $I$  the second moment of area. The subscripts  $c$  and  $s$  denote element concrete and steel beam, respectively.  $M(x)$  is the bending moment while and are the distances from the bottom of the concrete slab and the top of the steel beam to their respective centric.

$\varepsilon_c^{(M)}$  and  $\varepsilon_s^{(M)}$  are the unknowns longitudinal strains of the concrete and steel beam, respectively, at the adhesive interface and they are due to the longitudinal forces. These strains are given as follow

$$\varepsilon_c^{(N)}(x) = \frac{du_c^{(N)}(x)}{dx} \quad (5)$$

$$\varepsilon_s^{(N)}(x) = \frac{du_s^{(N)}(x)}{dx} \quad (6)$$

Where  $u_c^{(N)}(x)$  and  $u_s^{(N)}(x)$  represents the longitudinal force-induced adhesive displacement at the interface between the upper the concrete slab and the adhesive, also at the interface between the lower the steel beam and the adhesive.

To determine the unknowns longitudinal strains  $\varepsilon_c^{(N)}$  and  $\varepsilon_s^{(N)}$ , shear deformations of the adherents are incorporated in this analysis. It is reasonable to assume that the shear stresses, which develop are continuous across the adhesive–adherent interface. In addition, equilibrium requires the shear stress be zero at the free surface. Using the same methodology developed by Tsai *et al* (1998) this effect is taken into account. A parabolic variation of longitudinal displacements  $U_c^{(N)}(x, y)$  and  $U_s^{(N)}(x, y)$  in both adherents (concrete slab and steel beam) is assumed.

$$U_c^{(N)}(x, y) = A_1(x)y^2 + B_1(x)y + C_1(x) \quad (7)$$

$$U_s^{(N)}(x, y) = A_2(x)y'^2 + B_2(x)y' + C_2(x) \quad (8)$$

Where  $y(y')$  is a local coordinate system with the origin at the top surface of the upper lower adherent Fig. 2.

The shear stresses in the two adherents are given by

$$\sigma_{xy(c)} = G_c \gamma_{xy(c)} \quad (9)$$

$$\sigma_{xy'(s)} = G_s \gamma_{xy'(s)} \quad (10)$$

With

$$\gamma_{xy(c)} = \frac{dU_c^{(N)}}{dy} + \frac{dW_c^{(N)}}{dx} \quad (11)$$

$$\gamma_{xy(s)} = \frac{dU_s^{(N)}}{dy} + \frac{dW_s^{(N)}}{dx} \quad (12)$$

$G_c$  and  $G_s$  are the transverse shear moduli of the concrete slab and steel beam, respectively. Neglecting the variations of transverse displacement  $W_c^{(N)}$  and  $W_s^{(N)}$  (induced by the longitudinal forces) with the longitudinal coordinate  $x$ .

$$\gamma_{xy(c)} \approx \frac{dU_c^{(N)}}{dy} \quad (13)$$

$$\gamma_{xy(s)} \approx \frac{dU_s^{(N)}}{dy} \quad (14)$$

And the shear stresses are expressed as

$$\sigma_{xy(c)} = G_c(2A_1y + B_1) \quad (15)$$

$$\sigma_{xy(s)} = G_s(2A_2y' + B_2) \quad (16)$$

The shear stresses must satisfy the following conditions

$$\sigma_{xy(c)}(x, t_c) = \sigma_{xy(s)}(x, 0) = \tau(x) = \tau_a \quad (17)$$

$$\sigma_{xy(c)}(x, 0) = 0, \quad \sigma_{xy'(s)}(x, t_s) = 0 \quad (18)$$

$t_c$ ,  $t_s$  are the thickness of the concrete slab and steel beam, respectively.

Condition (17) follows from continuity and the assumption of the uniform shear stresses ( $\tau(x) = \tau_a$ ) through of adhesive. Condition (18) states there is no shear stresses at the top surface of the concrete slab (i.e., at  $y = 0$ ) and at the bottom surface at the steel beam (i.e., at  $y' = t_s$ ). These conditions yield

$$\sigma_{xy(c)} = \frac{\tau(x)}{t_c}y \quad (19)$$

$$\sigma_{xy(s)} = \left(1 - \frac{y'}{t_s}\right)\tau(x) \quad (20)$$

Then with a linear material constitutive relationship the element shear strain for the concrete slab and for the steel beam are written as

$$y_{xy(c)} = y_c = \left( \frac{\tau_a}{G_c t_c} \right) y \quad (21)$$

$$y_{xy(s)} = \left( 1 - \frac{y'}{t_s} \right) \frac{\tau_a}{G_s} \quad (22)$$

The longitudinal displacement functions  $U_c^{(N)}$  for the upper concrete slab and  $U_s^{(N)}$  for the lower steel beam, due to the longitudinal forces, are given by

$$U_c^{(N)}(y) = U_c^{(N)}(0) + \int_0^y y_c(y) dy = U_c^{(N)}(0) + \frac{\tau_a}{2G_c t_c} y^2 \quad (23)$$

$$U_s^{(N)}(y') = u_s^{(N)} + \int_0^{y'} y_s(y') dy' = u_s^{(N)} + \left( y' + \frac{y'^2}{2t_s} \right) \tau_a \quad (24)$$

Where  $(U_c^{(N)}(0))$  represents the displacement at the top surface of the upper adherend (due to the longitudinal forces) and  $u_s^{(N)}$  is the longitudinal force-induced adhesive displacement at the interface between the adhesive and lower adherend.

Note that due to the perfect bonding of the joints, the displacements are continuous at the interfaces between the adhesive and adherends. As a result, the  $u_s^{(N)}$  should be equivalent to the lower adherend displacement at the interface and  $u_c^{(N)}$  (the displacement at the interface between the adhesive and upper adherend) should be the same as the upper adherend displacement at the interface. Based on Eq. (23) the  $u_c^{(N)}$  can be expressed as

$$u_c^{(N)} = U_c^{(N)}(y = t_c) = U_c^{(N)}(0) + \frac{\tau_a t_c}{2G_c} \quad (25)$$

Using Eq. (25), Eq. (23) can be rewritten as

$$U_c^{(N)}(y) = u_c^{(N)} + \frac{\tau_a}{2G_c t_c} y^2 + \frac{\tau_a t_c}{2G_c} \quad (26)$$

The longitudinal resultant force, for the upper concrete slab is

$$N_c = b_c \int_0^{t_c} \sigma_c^N(y) dy \quad (27)$$

And the longitudinal resultant force,  $N_s$  for the lower steel beam having an I-section view Fig. 1 can be written

$$N_s^N = b_s \int_0^{t_a} \sigma_s^N(y') dy' + b_0 \int_{t_0}^{t_a - t_0} \sigma_s^N(y') dy' + \int_{t_s - t_0}^{t_s} \sigma_s^N(y') dy' \quad (28)$$

Where  $\sigma_c^N$  and  $\sigma_s^N$  are longitudinal normal stresses for the upper and lower adherends, respectively. By changing these stresses into functions of displacements and substituting Eqs. (24) and (26) into the displacements, Eqs. (27) and (28) can be rewritten as

$$N_c = E_c b_c \int_0^{t_c} \frac{dU_c^{(N)}}{dx} dy = E_c A_c \left( \frac{dU_c^{(N)}}{dx} - \frac{t_c d\tau_a}{3G_c dx} \right) \quad (29)$$

And

$$\begin{aligned} N_s &= E_s \left( b_s \int_0^{t_0} \frac{dU_s^{(N)}}{dx} dy' + b_0 \int_{t_0}^{t_a-t_0} \frac{dU_s^{(N)}}{dx} dy' + b_s \int_{t_a-t_0}^{t_s} \frac{dU_s^{(N)}}{dx} dy' \right) \\ &= E_s A_s \left[ \frac{dU_s^{(N)}}{dx} - \frac{1}{6G_s t_s} \left( b_s \left( (t_s - t_0)^3 - t_0^3 - t_s^3 + 6t_s^2 t_0 \right) \right. \right. \\ &\quad \left. \left. + b_0 \left( (3t_a^2(t_s - 2t_0) - (t_s - t_0)^2 + t_0^2) \right) \frac{d\tau(x)}{dx} \right] \right] \end{aligned} \quad (30)$$

Hence, the longitudinal strains induced by the longitudinal forces Eq. (4) can be expressed as

$$\varepsilon_c^{(N)} = \frac{du_c^{(N)}(x)}{dx} = \frac{N_c}{E_c A_c} + \frac{t_c d\tau_a}{3G_c dx} \quad (31)$$

$$\begin{aligned} \varepsilon_s^{(N)} &= \frac{du_s^{(N)}(x)}{dx} = \frac{N_s}{E_s A_s} + \frac{1}{6G_s t_s} \left( b_s \left( (t_s - t_0)^3 - t_0^3 - t_s^3 + 6t_s^2 t_0 \right) \right. \\ &\quad \left. + b_0 \left( (3t_a^2(t_s - 2t_0) - (t_s - t_0)^2 + t_0^2) \right) \frac{d\tau(x)}{dx} \right) \end{aligned} \quad (32)$$

Substituting Eqs. (31), (32), (3) and (4) into Eqs. (1) and (2), respectively, these latter become

$$\varepsilon_c^{(N)} = \frac{du_c^{(N)}(x)}{dx} = \frac{y_c}{E_c I_c} M_c(x) + \frac{N_c(x)}{E_c A_c} + \frac{t_c d\tau_a}{3G_c dx} \quad (33)$$

$$\begin{aligned} \varepsilon_s^{(N)} &= \frac{du_s^{(N)}(x)}{dx} = -\frac{y_s}{E_s I_s} M_s(x) + \frac{N_s(x)}{E_s A_s} + \frac{1}{6G_s t_s} \left( b_s \left( (t_s - t_0)^3 - t_0^3 - t_s^3 + 6t_s^2 t_0 \right) \right. \\ &\quad \left. + b_0 \left( (3t_a^2(t_s - 2t_0) - (t_s - t_0)^2 + t_0^2) \right) \frac{d\tau(x)}{dx} \right) \end{aligned} \quad (34)$$

Where  $N(x)$  are the axial forces in each element, the cross-sectional area. The shear stress in the adhesive can be expressed as follows

$$\tau_a = \tau(x) = K_s [u_c(x) - u_s(x)] \quad (35)$$

Where  $K_s = \frac{G_a}{t_a}$  is shear stiffness of the adhesive,  $G_a$  and  $t_a$  are shear modulus and thickness of the adhesive, respectively;  $u_c(x)$  and  $u_s(x)$  are the longitudinal displacements at the base of

concrete slab and the top of steel beam. Differentiating the above expression we obtain

$$\frac{d\tau(x)}{dx} = K_s \left[ \frac{du_c(x)}{dx} - \frac{du_s(x)}{dx} \right] \quad (36)$$

Consideration of horizontal equilibrium gives

$$\frac{dN_c(x)}{dx} = \tau(x) \quad (37)$$

$$\frac{dN_s(x)}{dx} = -\tau(x) \quad (38)$$

Where

$$N_c(x) = N(x) = \int_0^x \tau(x) \quad (39)$$

$$N_s(x) = -N(x) = -\int_0^x \tau(x) \quad (40)$$

The condition of equal curvatures in the beam and slab provides the relation

$$\varphi = \frac{M_c(x)}{E_c A_c} = \frac{M_s(x)}{E_s A_s} = \frac{M_c(x) + M_s(x)}{E_c A_c + E_s A_s} \quad (41)$$

Under a vertical load, the variation of the moment on a length  $dx$  is balanced by the shear force (which corresponds to the elementary beam theory where) combined with the action of the connection

$$dM_c(x) = V_c dx - \tau(x) y_c \quad (42)$$

$$dM_s(x) = V_s dx - \tau(x) y_s \quad (43)$$

Moment equilibrium of the differential segment of the plated beam in Fig. 2 gives

$$M_T(x) = M_c(x) + M_s(x) + N(y_c + y_s + t_a) \quad (44)$$

Substituting Eqs. (33), (34), (37) and (38) into Eq. (35) we have

$$\begin{aligned} \frac{d\tau(x)}{dx} = K_s \left[ \frac{y_c}{E_c I_c} M_c(x) - \frac{N_c(x)}{E_c A_c} - \frac{t_c}{3G_c} + \frac{y_s}{E_s I_s} M_s(x) + \frac{N_s(x)}{E_s A_s} \right. \\ \left. - \frac{1}{6G_s t_s A_s} \left( b_s ((t_s - t_0)^3 - t_0^3 - t_s^3 + 6t_s^2 t_0) \right. \right. \\ \left. \left. + b_0 \left( (3t_a^2 (t_s - 2t_0) - (t_s - t_0)^2 + t_0^2) \right) \frac{d\tau(x)}{dx} \right) \right] \quad (45) \end{aligned}$$

Deriving Eq. (45) once yields



$$\begin{aligned} \frac{d^2\tau(x)}{K_s \cdot dx^2} = & \left[ \frac{y_c}{E_c I_c} M_c(x) - \frac{N_c(x)}{E_c A_c} - \frac{t_c}{3G_c} + \frac{y_s}{E_s I_s} M_s(x) + \frac{N_s(x)}{E_s A_s} \right. \\ & - \frac{1}{6G_s t_s A_s} \left( b_s((t_s - t_0)^3 - t_0^3 - t_s^3 + 6t_s^2 t_0) \right. \\ & \left. \left. + b_0 \left( (3t_a^2(t_s - 2t_0) - (t_s - t_0)^2 + t_0^2) \right) \frac{d^2\tau(x)}{dx^2} \right) \right] \end{aligned} \quad (46)$$

Substitution of the shear forces (Eqs. (42) and (43)) and axial forces (Eqs. (37) and (38)) into Eq. (46) gives the following governing differential equation for the interfacial shear stress.

$$\begin{aligned} \frac{d^2\tau(x)}{K_s \cdot dx^2} - K_1 \left[ \frac{(y_c + y_s)(y_c + y_s + t_a)}{E_c I_c + E_s I_s} + \frac{1}{E_c A_c} + \frac{1}{E_s A_s} \right] \frac{d\tau(x)}{dx} \\ + K_1 \frac{(y_c + y_s)}{E_c I_c + E_s I_s} \cdot V_T(x) = 0 \end{aligned} \quad (47)$$

Where

$$K_1 = \frac{1}{\left( \frac{t_a}{G_a} + \frac{t_c}{3G_c} + \frac{t_s}{3G_s} \xi \right)} \quad (48)$$

And

$$\xi = \frac{1}{6G_s t_s A_s} \left( b_s((t_s - t_0)^3 - t_0^3 - t_s^3 + 6t_s^2 t_0) + b_0 \left( (3t_a^2(t_s - 2t_0) - (t_s - t_0)^2 + t_0^2) \right) \right) \quad (49)$$

For simplicity, the general solutions presented below are limited to loading which is either concentrated or uniformly distributed over part or the whole span of the beam, or both. For such loading,  $\frac{d^2 V_T(x)}{dx^2} = 0$ , and the general solution to Eq. (48) is given by simplified form

$$\tau(x) = \Delta_1 e^{\lambda \cdot x} + \Delta_2 e^{-\lambda \cdot x} + \delta \cdot V_T(x) \quad (50)$$

Where

$$\lambda = \sqrt{K_1 b_s \left[ \frac{(y_c + y_s)(y_c + y_s + t_a)}{E_c I_c + E_s I_s} + \frac{1}{E_c A_c} + \frac{1}{E_s A_s} \right]} \quad (51a)$$

$$\lambda^2 = K_1 b_s \left[ \frac{(y_c + y_s)(y_c + y_s + t_a)}{E_c I_c + E_s I_s} + \frac{1}{E_c A_c} + \frac{1}{E_s A_s} \right] \quad (51b)$$

$$\lambda^2 = \frac{b_s}{\left( \frac{t_a}{G_a} + \frac{t_c}{3G_c} + \frac{t_s}{3G_s} \xi \right)} \left[ \frac{(y_c + y_s)(y_c + y_s + t_a)}{E_c I_c + E_s I_s} + \frac{1}{E_c A_c} + \frac{1}{E_s A_s} \right] \quad (51c)$$

And

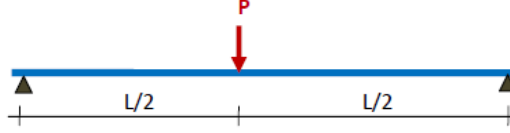


Fig. 3 Load definition

$$\delta = \frac{K_1}{\lambda^2} \left( \frac{1}{E_c A_c} + \frac{1}{E_s A_s} \right) = \frac{\frac{1}{E_c A_c} + \frac{1}{E_s A_s}}{\lambda^2 \left( \frac{t_a}{G_a} + \frac{t_c}{3G_c} + \frac{t_s}{3G_s} \xi \right)} \quad (52a)$$

$$\delta = \frac{\left( \frac{1}{E_c A_c} + \frac{1}{E_s A_s} \right)}{b_s \left[ \frac{(y_c + y_s)(y_c + y_s + t_a)}{E_c I_c + E_s I_s} + \frac{1}{E_c A_c} + \frac{1}{E_s A_s} \right]} \quad (52b)$$

$\Delta_1$  and  $\Delta_2$  are constant coefficients determined from the boundary conditions.

**Application for a composite steel-concrete beam in three-point bending:** In this paper, we are study a simply supported beams with a single load is concentrated in midspan Fig. 3, that  $\tau(x) = 0$  at  $x = \frac{L}{2}$ , and  $\frac{d\tau(x)}{dx} = 0$  at  $x = \frac{L}{2}$ , where L span length.

**Interfacial shear stress for a single point load:** For as  $0 \leq x \leq \frac{L}{2}$  as

$$\tau(x) = \frac{\delta \cdot P \cdot e^{(-\lambda \cdot \frac{L}{2} + \lambda \cdot x)}}{2 \cdot \left( e^{(-\lambda \cdot \frac{L}{2})} + e^{(\lambda \cdot \frac{L}{2})} \right)} - \frac{\delta \cdot P \cdot e^{(\lambda \cdot \frac{L}{2} - \lambda \cdot x)}}{2 \cdot \left( e^{(-\lambda \cdot \frac{L}{2})} + e^{(\lambda \cdot \frac{L}{2})} \right)} + \delta \cdot \frac{P}{2} \quad (53)$$

### 2.3 Normal stress distribution along the steel-concrete interface

The normal stress in the adhesive can be expressed as follows

$$\sigma(x) = K_n \cdot \Delta w(x) = K_n \cdot \left( \frac{dw_c(x)}{dx} - \frac{dw_s(x)}{dx} \right) \quad (54)$$

where  $K_n$  is normal stiffness of the adhesive per unit length and can be deduced as

$$K_n = \frac{\sigma(x)}{\Delta w(x)} = \frac{E_a}{t_a} \quad (55)$$

$(dw_c(x))$  and  $(dw_s(x))$  are the vertical displacements of concrete slab and steel beam, respectively.

Differentiating Eq. (54) twice results in

$$\frac{d^2 \sigma(x)}{d^2 \Delta w(x)} = K_n \cdot \left( \frac{d^2 w_c(x)}{dx^2} - \frac{d^2 w_s(x)}{dx^2} \right) \quad (56)$$

Considering the moment–curvature relationships for the concrete slab and the steel beam, respectively

$$\frac{d^2 w_c(x)}{dx^2} = -\frac{M_c(x)}{E_c I_c}, \quad \frac{d^2 w_s(x)}{dx^2} = -\frac{M_s(x)}{E_s I_s} \quad (57)$$

The equilibrium of concrete slab and steel beam, leads to the following relationships

$$\text{Concrete slab: } \frac{dM_c(x)}{dx} = V_c(x) - y_c \tau(x) \quad \text{and} \quad \frac{dV_c(x)}{dx} = -\sigma_n(x) - q \quad (58a)$$

$$\text{Steel beam: } \frac{dM_s(x)}{dx} = V_s(x) - y_s \tau(x) \quad \text{and} \quad \frac{dV_s(x)}{dx} = \sigma_n(x) \quad (58b)$$

Based on the above equilibrium equations, the governing differential equations for the deflection of concrete slab and steel beam, expressed in terms of the interfacial shear and normal stresses, are given as follows

$$\text{Concrete slab: } \frac{d^4 w_s(x)}{dx^4} = \frac{1}{E_c I_c} \sigma_n(x) + \frac{y_c}{E_c I_c} \frac{d\tau(x)}{dx} + \frac{q}{E_c I_c} \quad (59)$$

$$\text{Steel beam: } \frac{d^4 w_s(x)}{dx^4} = \frac{1}{E_s I_s} \sigma_n(x) + \frac{y_s}{E_s I_s} \frac{d\tau(x)}{dx} \quad (60)$$

Substitution of Eqs. (57) and (58) into the fourth derivation of the interfacial normal stress obtainable from Eq. (59) gives the following governing differential equation for the interfacial normal stress

$$\frac{d^4 \sigma_n(x)}{dx^4} + K_n \cdot b_s \left( \frac{1}{E_c I_c} + \frac{1}{E_s I_s} \right) \cdot \sigma_n(x) + K_n \cdot b_s \left( \frac{y_c}{E_c I_c} - \frac{y_s}{E_s I_s} \right) \cdot \frac{d\tau(x)}{dx} + K_n \cdot \frac{q}{E_c I_c} \quad (61)$$

The general solution to this fourth-order differential equation is

$$\begin{aligned} \sigma_n(x) = & e^{-\beta \cdot x} [\Delta_3 \cos(\beta \cdot x) + \Delta_4 \sin(\beta \cdot x)] \\ & + e^{\beta \cdot x} [\Delta_5 \cos(\beta \cdot x) + \Delta_6 \sin(\beta \cdot x)] - \mu_1 \cdot \frac{d\tau(x)}{dx} - \mu_2 q \end{aligned} \quad (62a)$$

For large values of  $x$  it is assumed that the normal stress approaches zero, and as a result  $\Delta_5 = \Delta_6 = 0$ . The general solution therefore becomes, where

$$\sigma_n(x) = e^{-\beta \cdot x} [\Delta_3 \cos(\beta \cdot x) + \Delta_4 \sin(\beta \cdot x)] - \mu_1 \cdot \frac{d\tau(x)}{dx} - \mu_2 q \quad (62b)$$

$$\sigma_n(x) = e^{-\beta \cdot x} [\Delta_3 \cos(\beta \cdot x) + \Delta_4 \sin(\beta \cdot x)] - \left( \frac{y_c}{E_c I_c} - \frac{y_s}{E_s I_s} \right) \cdot \frac{d\tau(x)}{dx} - \left( \frac{E_s I_s}{E_c I_c + E_s I_s} \right) q \quad (62c)$$

$$\beta = \sqrt[4]{\frac{K_n \cdot b_s \left( \frac{1}{E_c I_c} + \frac{1}{E_s I_s} \right)}{4}} \quad (63)$$

$$\mu_1 = \left( \frac{y_c}{E_c I_c} - \frac{y_s}{E_s I_s} \right) \quad (64)$$

and

$$\mu_2 = \left( \frac{E_s I_s}{E_c I_c + E_s I_s} \right) \quad (65)$$

$\Delta_3$  and  $\Delta_4$  are constant coefficients determined from the boundary conditions.

**Interfacial normal stress for a single point load:** As is described by Smith and Teng (2002), the constants  $\Delta_3$  and  $\Delta_4$  in Eq. (62c) are determined using the appropriate boundary conditions (Fig. 3) and they are written as follow

$$\sigma_n(x) = e^{-\beta \cdot x} [\Delta_3 \cos(\beta \cdot x) + \Delta_4 \sin(\beta \cdot x)] - \left( \frac{y_c}{E_c I_c} - \frac{y_s}{E_s I_s} \right) \cdot \frac{d\tau(x)}{dx} - \left( \frac{E_s I_s}{E_c I_c + E_s I_s} \right) q \quad (66)$$

$$\Delta_3 = \frac{E_a}{2 \cdot \beta^2 t_a E_c I_c} [V_T(0) + \beta M_T(0)] - \frac{\mu_3}{2 \cdot \beta^2} \tau(0) + \frac{\mu_1}{2 \cdot \beta^2} \left[ \frac{d^4 \tau(0)}{dx^4} + \beta \frac{d^2 \tau(0)}{dx^2} \right] \quad (67)$$

$$\Delta_4 = \frac{E_a}{2 \cdot \beta^2 t_a E_c I_c} M_T(0) - \frac{n_1}{2 \cdot \beta^2} \frac{d^2 \tau(0)}{dx^2} \quad (68)$$

$$\mu_3 = \frac{E_a \cdot b_s}{t_a} \left( \frac{y_c}{E_c I_c} + \frac{y_s}{E_s I_s} \right) \quad (69)$$

The above expressions for the constants  $\Delta_3$  and  $\Delta_4$  have been left in terms of the bending moment  $M_T(0)$  and shear force  $V_T(0)$  at the end of the adherends. With the constants  $\Delta_3$  and  $\Delta_4$  determined, the interfacial normal stress can then be found using Eq. (63).

#### 2.4 Slip distribution along the steel–concrete interface

The relative slip strain at the interface is calculated as

$$\frac{dS(x)}{dx} = \frac{du_c(x)}{dx} - \frac{du_s(x)}{dx} = \varepsilon_c(x) - \varepsilon_s(x) \quad (70)$$

As noted in the assumptions, the slip of adhesive is proportional to the shear force,  $\tau(x)$  which the connector transmitted. The constant of proportionality is the adhesive stiffness  $K_a$ .

The shear stress in the adhesive can be expressed as follows

$$\tau_a = \tau(x) = K_s [u_c(x) - u_s(x)] \Leftrightarrow \tau(x) = K_s \cdot S(x) \quad (71)$$

$$S(x) = \frac{1}{K_s} \tau(x) = \frac{t_a}{G_a} (\Delta_1 e^{\lambda \cdot x} + \Delta_2 e^{-\lambda \cdot x} + \delta \cdot V_T(x)) \tag{72}$$

Where  $S(x)$  represent slip between adhrsnds and  $K_s = \frac{G_a}{t_a}$  is shear stiffness of the adhesive,  $G_a$  and  $t_a$  are shear modulus and thickness of the adhesive.

**Slip interfacial for a single point load:** For the case of simply supported beams with a single load shown in Fig. 3, the slip due to load is

$$S(x) = \frac{\delta \cdot P}{2} \left[ \frac{e^{-\lambda \frac{L}{2} + \lambda \cdot x}}{(e^{-\lambda \frac{L}{2}} + e^{\lambda \frac{L}{2}})} - \frac{\delta \cdot P \cdot e^{\lambda \frac{L}{2} - \lambda \cdot x}}{2(e^{-\lambda \frac{L}{2}} + e^{\lambda \frac{L}{2}})} + 1 \right] \tag{73}$$

### 3. Results: discussion and analysis

#### 3.1 Validation of analytical model and discussions

The analytical model elastic developed herein has been used to analyze a simply supported composite beam (P3) tested by Bouazaoui *et al.* (2007) with two types different (Sikadur 30 and Sikaforce 7750), the results are compared with corresponding experimental data in this section. The span of the composite beam under a point load was 3.3 m, and Fig. 4 illustrates the dimensions of

Table 1 Material properties of the composite beam

	Young's Modulus (MPa)	Tensile or compression strength (MPa)	Ratio of poisson
Steel Beam: IPE220	205 000	470	0,3
Concrete Slab	36 600	68	0,28
Adhesives: Sikadur 30	12300	19,5	0,34
Adhesives: Sikaforce 7750	80	9,2	0,38

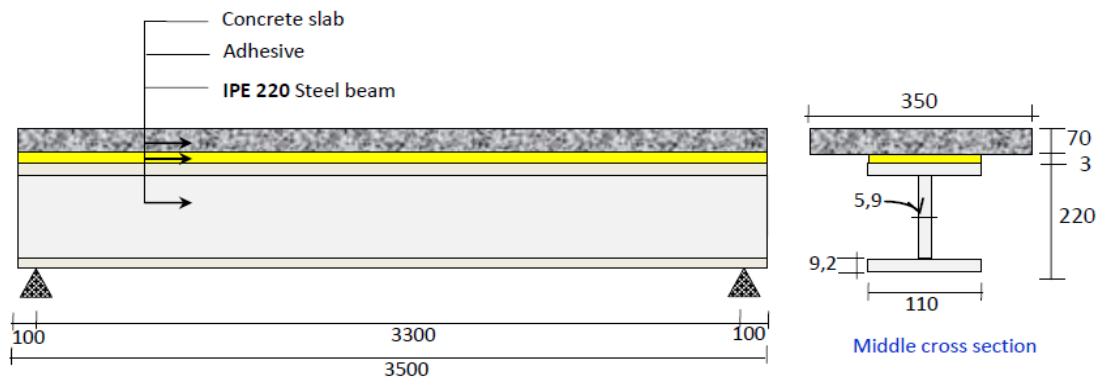


Fig. 4 Simply supported composite beam

this composite beam. The material properties of the composite beam are listed below (Table 1).

To test and validate our proposed analytical model, we compared our results of slip with those of the experimental data given by Bouzaoui *et al.* (2007) in Reims university, for a simply supported of a new mode of assembly of composite steel-concrete beams.

Fig. 5 show a comparison between the results of the present analytical with the experimental data study of composite steel-concrete beams assembly with two types different of adhesives (Sikadure and Sikaforce) and the thickness adhesive 3 mm. The comparison of experimental results with those given by our analytical model in the elastic range shows a good agreement between the curves. This confirms the validation of our model.

**3.2 The results of the interfacial shear stress:**

Once, our analytical model is validated by comparison with experimental tests by Bouzaoui *et al.* (2007); so we can use our model to calculate the shear stress at the interface of the composite steel-concrete beam assembled with an adhesive joint. The following Fig. 6 represent the results of

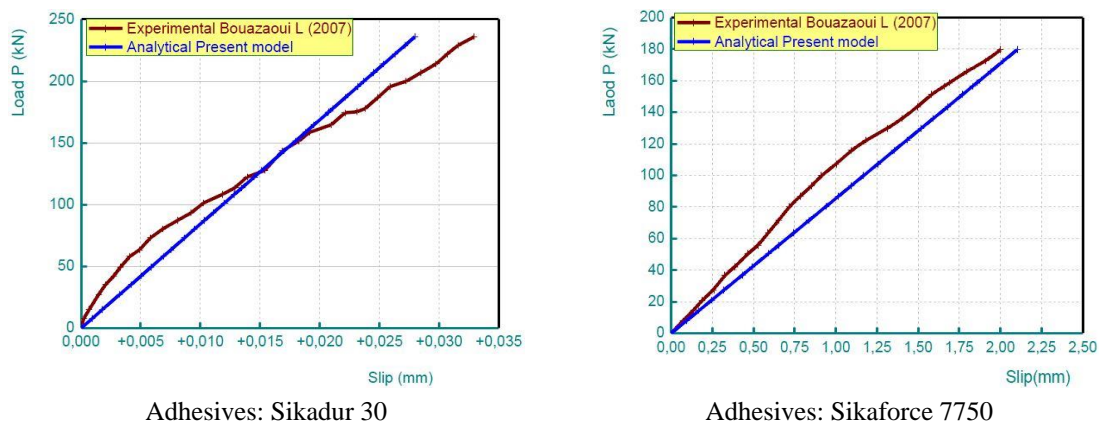


Fig. 5 Load–slip curves of composite steel-concrete beam

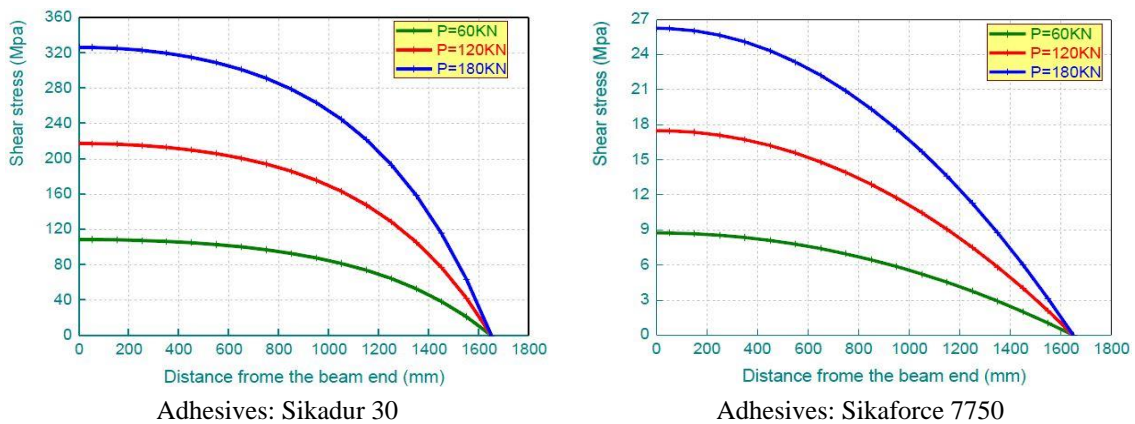


Fig. 6 Distribution of shear stress along span from composite steel-concrete beam

the shear stress at the interface of composite steel-concrete beams with two types different of adhesives joints Sikadure and Sikaforce respectively under these loads 100 kN, 200 kN and 300 kN.

### 3.3 Interfacial stresses for different parameters

We propose in this section a parametric study applied the proposed model; we take the same beam geometry studied for validation but with deferent thickness of the adhesive layer (Sikadure and Sikaforce).

**Interfacial stresses and slips for different parameters:** In this section, numerical results of the present solution are presented to study the effect of various parameters on the distributions of the interfacial stresses and slip in a composite steel concrete beam assembly with Sikadure or Sikaforce is subjected to a single load 200 kN. These results are intended to demonstrate the main characteristics of interfacial stress and slip distributions in these composite beams. The numerical results are presented in Figs. 7 and 8. The effect of the thickness of the adhesive layer ( $t_a = 1, 2$  and

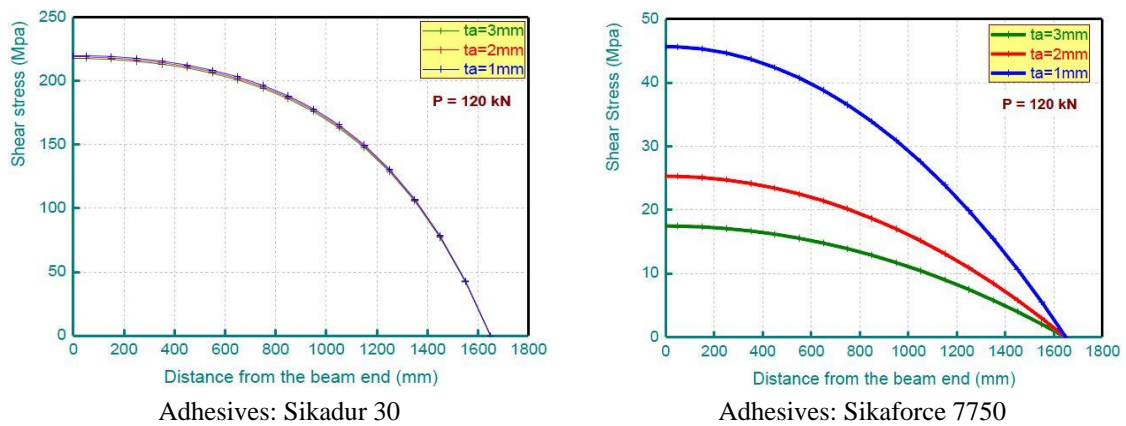


Fig. 7 Effect of the thickness of the adhesive on shear stress along span slip

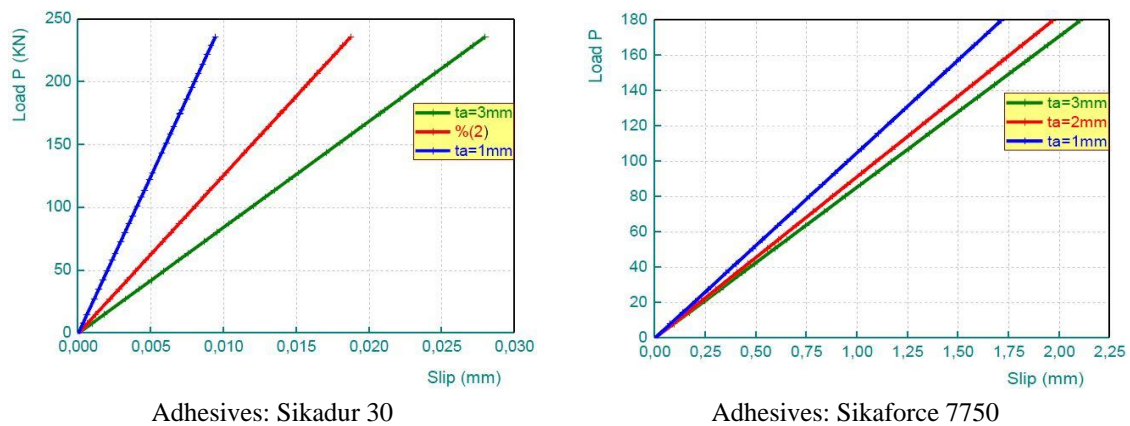


Fig. 8 Influence of the thickness of the adhesive on slip

3 mm, respectively) on interfacial shear stresses is shown in Fig. 7, and the effect of the thickness of the adhesive layer ( $t_a = 1, 2$  and  $3$  mm, respectively) on interfacial slip is shown in Fig. 8. It can be seen from Figs. 7 and 8 that the thickness of adhesive layer affects the slip and shear stress concentrations, hardly the stress levels. However, design of the properties and thickness of the adhesive is a difficult problem. An optimization design of the adhesive is expected.

#### 4. Conclusions

This paper presents an improved solution for interfacial stresses and slip in a composite steel concrete beam bonded with an adhesive including the effect of transverse shear deformation in both the steel beam and concrete slab in the theoretical analyses by assuming linear shear stress distributions through the thickness of the adherend. The classical solutions which neglect the adherend shear deformations. In these cases the effect of the shear deformations becomes significant and has to be addressed in design; the analytical advantage of this improvement is possible to determine the shear stress to estimate exact prediction of shear stress interfacial along span between concrete slab and steel beam. The exact prediction of these stresses will be very important to make an accurate analysis of the mode of fracture. Closed-form solutions are obtained for composite steel-concrete beams simply supported at both ends and verified through direct comparisons with by Bouazaoui *et al.* (2007). A parametric study is then conducted, evaluating the effect of transverse shear deformation on the interfacial stresses and slip with varying material and geometry parameters of the adhesive. The results were satisfactory compared with existing experimental results and therefore constitute a first step in the proposed solutions for the assembly of composite steel-concrete beams by gluing and this research is helpful for the understanding on mechanical behavior of the connection and design of such structures.

#### Acknowledgments

This research was supported by the Algerian Ministry of Higher Education and Scientific Research (MESRS) as part of the grant for the PRFU research project n° A01L02UN140120200002 and by the University of Tiaret, in Algeria.

#### References

- Abdelhak, Z., Hadji, L., Khelifa, Z., Hassaine Daouadji, T. and Adda Bedia, E.A. (2016), "Analysis of buckling response of functionally graded sandwich plates using a refined shear deformation theory", *Wind Struct.*, **22**(3), 291-305. <https://doi.org/10.12989/was.2016.22.3.291>
- Abderezak, R., Daouadji, T.H., Rabia, B. and Belkacem, A. (2018a), "Nonlinear analysis of damaged RC beams strengthened with glass fiber reinforced polymer plate under symmetric loads", *Earthq. Struct., Int. J.*, **15**(2), 113-122. <https://doi.org/10.12989/eas.2018.15.2.113>
- Abderezak, R., Daouadji, T.H., Abbas, B., Rabia, B., Belkacem, A. and Abbas, F. (2018b), "Elastic analysis of interfacial stress concentrations in CFRP-RC hybrid beams: Effect of creep and shrinkage", *Adv. Mater. Res., Int. J.*, **6**(3), 257-278. <https://doi.org/10.12989/amr.2017.6.3.257>
- Abderezak, R., Rabia, B., Daouadji, T.H., Abbas, B., Belkacem, A. and Abbas, F. (2019), "Elastic analysis of interfacial stresses in prestressed PFGM-RC hybrid beams", *Adv. Mater. Res., Int. J.*, **7**(2), 83-103.



- <https://doi.org/10.12989/amr.2018.7.2.083>
- Abualnour, M., Chikh, A., Hebali, H., Kaci, A., Tounsi, A., Bousahla, A.A. and Tounsi, A. (2019), "Thermomechanical analysis of antisymmetric laminated reinforced composite plates using a new four variable trigonometric refined plate theory", *Comput. Concrete, Int. J.*, **24**(6), 489-498.  
<https://doi.org/10.12989/cac.2019.24.6.489>
- Addou, F.Y., Meradjah, M., Bousahla, A.A., Benachour, A., Bourada, F., Tounsi, A. and Mahmoud, S.R. (2019), "Influences of porosity on dynamic response of FG plates resting on Winkler/Pasternak/Kerr foundation using quasi 3D HSDT", *Comput. Concrete, Int. J.*, **24**(4), 347-367.  
<https://doi.org/10.12989/cac.2019.24.4.347>
- Adim, B. and Daouadji, T.H. (2016), "Effects of thickness stretching in FGM plates using a quasi-3D higher order shear deformation theory", *Adv. Mater. Res., Int. J.*, **5**(4), 223-244.  
<https://doi.org/10.12989/amr.2016.5.4.223>
- Adim, B., Daouadji, T.H. and Abbes, B. (2016a), "Buckling analysis of anti-symmetric cross-ply laminated composite plates under different boundary conditions", *Int. Appl. Mech.*, **52**(6), 126-141.  
<https://doi.org/10.1007/s10778-016-0787-x>
- Adim, B., Daouadji, T.H., Rabia, B. and Hadji, L. (2016b), "An efficient and simple higher order shear deformation theory for bending analysis of composite plates under various boundary conditions", *Earthq. Struct., Int. J.*, **11**(1), 63-82. <https://doi.org/10.12989/eas.2016.11.1.063>
- Adim, B., Daouadji, T.H., Abbes, B. and Rabahi, A. (2016c), "Buckling and free vibration analysis of laminated composite plates using an efficient and simple higher order shear deformation theory", *Mech. Ind.*, **17**, 512. <https://doi.org/10.1051/meca/2015112>
- Adim, B., Daouadji, T.H. and Rabahi, A. (2016d), "A simple higher order shear deformation theory for mechanical behavior of laminated composite plates", *IJAS, Int. J. Adv. Struct. Eng.*, **8**, 103-117.  
<https://doi.org/10.1007/s40091-016-0109-x>
- Alimirzaei, S., Mohammadimehr, M. and Tounsi, A. (2019), "Nonlinear analysis of viscoelastic micro-composite beam with geometrical imperfection using FEM: MSGT electro-magneto-elastic bending, buckling and vibration solutions", *Struct. Eng. Mech., Int. J.*, **71**(5), 485-502.  
<https://doi.org/10.12989/sem.2019.71.5.485>
- Balubaid, M., Tounsi, A., Dakhel, B. and Mahmoud, S.R. (2019), "Free vibration investigation of FG nanoscale plate using nonlocal two variables integral refined plate theory", *Comput. Concrete, Int. J.*, **24**(6), 579-586. <https://doi.org/10.12989/cac.2019.24.6.579>
- Belbachir, N., Draich, K., Bousahla, A.A., Bourada, M., Tounsi, A. and Mohammadimehr, M. (2019), "Bending analysis of anti-symmetric cross-ply laminated plates under nonlinear thermal and mechanical loadings", *Steel Compos. Struct., Int. J.*, **33**(1), 81-92. <https://doi.org/10.12989/scs.2019.33.1.081>
- Belbachir, N., Bourada, M., Draiche, K., Tounsi, A., Bourada, F., Bousahla, A.A. and Mahmoud, S.R. (2020), "Thermal flexural analysis of anti-symmetric cross-ply laminated plates using a four variable refined theory", *Smart Struct. Syst., Int. J.*, **25**(4), 409-422. <https://doi.org/10.12989/sss.2020.25.4.409>
- Belkacem, A., Tahar, H.D., Abderrezak, R., Amine, B.M., Mohamed, Z. and Boussad, A. (2018), "Mechanical buckling analysis of hybrid laminated composite plates under different boundary conditions", *Struct. Eng. Mech., Int. J.*, **66**(6), 761-769. <https://doi.org/10.12989/sem.2018.66.6.761>
- Benachour, A., Benyoucef, S. and Tounsi, A. (2008), "Interfacial stress analysis of steel beams reinforced with bonded prestressed FRP plate", *Eng. Struct.*, **30**, 3305-3315.  
<https://doi.org/10.1016/j.engstruct.2008.05.007>
- Benferhat, R., Daouadji, T.H. and Adim, B. (2016a), "A novel higher order shear deformation theory based on the neutral surface concept of FGM plate under transverse load", *Adv. Mater. Res., Int. J.*, **5**(2), 107-120.  
<https://doi.org/10.12989/amr.2016.5.2.107>
- Benferhat, R., Daouadji, T.H., Mansour, M.S. and Hadji, L. (2016b), "Effect of porosity on the bending and free vibration response of functionally graded plates resting on Winkler-Pasternak foundations", *Earthq. Struct., Int. J.*, **10**(5), 1429-1449. <https://doi.org/10.12989/eas.2016.10.5.1033>
- Benferhat, R., Daouadji, T.H. and Mansour, M.S. (2016c), "Free vibration analysis of FG plates resting on the elastic foundation and based on the neutral surface concept using higher order shear deformation theory",

- Comptes Rendus Mecanique*, **344**(9), 631-641. <https://doi.org/10.1016/j.crme.2016.03.002>
- Benferhat, R., Hassaine Daouadji, T., Hadji, L. and Said Mansour, M. (2016d), "Static analysis of the FGM plate with porosities", *Steel Compos. Struct., Int. J.*, **21**(1), 123-136. <https://doi.org/10.12989/scs.2016.21.1.123>
- Benhenni, M.A., Daouadji, T.H., Abbes, B., Adim, B., Li, Y. and Abbes, F. (2018), "Dynamic analysis for anti-symmetric cross-ply and angle-ply laminates for simply supported thick hybrid rectangular plates", *Adv. Mater. Res., Int. J.*, **7**(2), 83-103. <https://doi.org/10.12989/amr.2018.7.2.119>
- Benhenni, M.A., Daouadji, T.H., Abbes, B., Abbes, F., Li, Y. and Adim, B. (2019a), "Numerical analysis for free vibration of hybrid laminated composite plates for different boundary conditions", *Struct. Eng. Mech., Int. J.*, **70**(5), 535-549. <https://doi.org/10.12989/sem.2019.70.5.535>
- Benhenni, M.A., Adim, B., Daouadji, T.H., Abbès, B., Abbès, F., Li, Y. and Bouzidane, A. (2019b), "A comparison of closed form and finite element solutions for the free vibration of hybrid cross ply laminated plates", *Mech. Compos. Mater.*, **55**(2), 181-194. <https://doi.org/10.1007/s11029-019-09803-2>
- Bensattalah, T., Daouadji, T.H., Zidour, M., Tounsi, A. and Bedia, E.A. (2016), "Investigation of thermal and chirality effects on vibration of single walled carbon nanotubes embedded in a polymeric matrix using nonlocal elasticity theories", *Mech. Compos. Mater.*, **52**(4), 555-568. <https://doi.org/10.1007/s11029-016-9606-z>
- Bensattalah, T., Zidour, M. and Daouadji, T.H. (2018), "Analytical analysis for the forced vibration of CNT surrounding elastic medium including thermal effect using nonlocal Euler-Bernoulli theory", *Adv. Mater. Res., Int. J.*, **7**(3), 163-174. <https://doi.org/10.12989/amr.2018.7.3.163>
- Berghouti, H., Adda Bedia, E.A., Benkhedda, A. and Tounsi, A. (2019), "Vibration analysis of nonlocal porous nanobeams made of functionally graded material", *Adv. Nano Res., Int. J.*, **7**(5), 351-364. <https://doi.org/10.12989/anr.2019.7.5.351>
- Bouazaoui, L., Perrenot, G., Delmas, Y. and Li, A. (2007), "Experimental study of bonded steel concrete composite structures", *J. Constr. Steel Res.*, **63**, 1268-1278. <http://dx.doi.org/10.1016/j.jcsr.2006.11.002>
- Bouakaz, K., Daouadji, T.H., Meftah, S.A., Ameer, M., Tounsi, A. and Bedia, E.A. (2014), "A Numerical analysis of steel beams strengthened with composite materials", *Mech. Compos. Mater.*, **50**(4), 685-696. <https://doi.org/10.1007/s11029-014-9435-x>
- Boulefrakh, L., Hebali, H., Chikh, A., Bousahla, A.A., Tounsi, A. and Mahmoud, S.R. (2019), "The effect of parameters of visco-Pasternak foundation on the bending and vibration properties of a thick FG plate", *Geomech. Eng., Int. J.*, **18**(2), 161-178. <https://doi.org/10.12989/gae.2019.18.2.161>
- Bousahla, A.A., Bourada, F., Mahmoud, S.R., Tounsi, A., Algarni, A., Bedia, E.A. and Tounsi, A. (2020), "Buckling and dynamic behavior of the simply supported CNT-RC beams using an integral-first shear deformation theory", *Comput. Concrete, Int. J.*, **25**(2), 155-166. <https://doi.org/10.12989/cac.2020.25.2.155>
- Boussoula, A., Boucham, B., Bourada, M., Bourada, F., Tounsi, A., Bousahla, A.A. and Tounsi, A. (2020), "A simple nth-order shear deformation theory for thermomechanical bending analysis of different configurations of FG sandwich plates", *Smart Struct. Syst., Int. J.*, **25**(2), 197-218. <https://doi.org/10.12989/sss.2020.25.2.197>
- Boukhlif, Z., Bouremana, M., Bourada, F., Bousahla, A.A., Bourada, M., Tounsi, A. and Al-Osta, M.A. (2019), "A simple quasi-3D HSDT for the dynamics analysis of FG thick plate on elastic foundation", *Steel Compos. Struct., Int. J.*, **31**(5), 503-516. <https://doi.org/10.12989/scs.2019.31.5.503>
- Boutaleb, S., Benrahou, K.H., Bakora, A., Algarni, A., Bousahla, A.A., Tounsi, A., Tounsi, A. and Mahmoud, S.R. (2019), "Dynamic analysis of nanosize FG rectangular plates based on simple nonlocal quasi 3D HSDT", *Adv. Nano Res., Int. J.*, **7**(3), 191-208. <https://doi.org/10.12989/anr.2019.7.3.191>
- Chaabane, L.A., Bourada, F., Sekkal, M., Zerouati, S., Zaoui, F.Z., Tounsi, A., Derras, A., Bousahla, A.A. and Tounsi, A. (2019), "Analytical study of bending and free vibration responses of functionally graded beams resting on elastic foundation", *Struct. Eng. Mech., Int. J.*, **71**(2), 185-196. <https://doi.org/10.12989/sem.2019.71.2.185>
- Chedad, A., Daouadji, T.H., Abderezak, R., Belkacem, A., Abbes, B., Rabia, B. and Abbes, F. (2018), "A high-order closed-form solution for interfacial stresses in externally sandwich FGM plated RC beams", *Adv.*

- Mater. Res., Int. J.*, **6**(4), 317-328. <https://doi.org/10.12989/amr.2017.6.4.317>
- Chen, J., Zhang, H. and Yu, Q.Q. (2019), "Static and fatigue behavior of steel-concrete composite beams with corroded studs", *J. Constr. Steel Res.*, **156**, 18-27. <https://doi.org/10.1016/j.jcsr.2019.01.019>
- Daouadji, T.H. (2013), "Analytical analysis of the interfacial stress in damaged reinforced concrete beams strengthened by bonded composite plates", *Strength Mater.*, **45**(5), 587-597. <https://doi.org/10.1007/s11223-013-9496-4>
- Daouadji, T.H. (2016c), "Theoretical analysis of composite beams under uniformly distributed load", *Adv. Mater. Res., Int. J.*, **5**(1), 1-9. <https://doi.org/10.12989/amr.2016.5.1.001>
- Daouadji, T.H. (2017), "Analytical and numerical modeling of interfacial stresses in beams bonded with a thin plate", *Adv. Computat. Des., Int. J.*, **2**(1), 57-69. <https://doi.org/10.12989/acd.2017.2.1.057>
- Daouadji, T.H. and Adim, B. (2016c), "An analytical approach for buckling of functionally graded plates", *Adv. Mater. Res., Int. J.*, **5**(3), 141-169. <https://doi.org/10.12989/amr.2016.5.3.141>
- Daouadji, T.H. and Benferhat, R. (2016a), "Bending analysis of an imperfect FGM plates under hygro-thermo-mechanical loading with analytical validation", *Adv. Mater. Res., Int. J.*, **5**(1), 35-53. <https://doi.org/10.12989/amr.2016.5.1.035>
- Daouadji, H.T., Benyoucef, S., Tounsi, A., Benrahou, K.H. and Bedia, A.E. (2008), "Interfacial stress concentrations in FRP-damaged RC hybrid beams", *Compos. Interf.*, **15**(4), 425-440. <https://doi.org/10.1163/156855408784514702>
- Daouadji, T.H., Rabahi, A., Abbes, B. and Adim, B. (2016a), "Theoretical and finite element studies of interfacial stresses in reinforced concrete beams strengthened by externally FRP laminates plate", *J. Adhes. Sci. Technol.*, **30**(12), 1253-1280. <https://doi.org/10.1080/01694243.2016.1140703>
- Daouadji, T.H., Chedad, A. and Adim, B. (2016b), "Interfacial stresses in RC beam bonded with a functionally graded material plate", *Struct. Eng. Mech., Int. J.*, **60**(4), 693-705. <http://dx.doi.org/10.12989/sem.2016.60.4.693>
- Daouadji, H.T., Benyoucef, S., Tounsi, A., Benrahou, K.H. and Bedia, A.E. (2016c), "Elastic analysis effect of adhesive layer characteristics in steel beam strengthened with a fiber-reinforced polymer plates", *Struct. Eng. Mech., Int. J.*, **59**(1), 83-100. <https://doi.org/10.12989/sem.2016.59.1.083>
- Daouadji, T.H., Benferhat, R. and Adim, B. (2016d), "Bending analysis of an imperfect advanced composite plates resting on the elastic foundations", *Coupl. Syst. Mech., Int. J.*, **5**(3), 269-285. <https://doi.org/10.12989/csm.2016.5.3.269>
- Dezi, L., Ianni, C. and Tarantino, A.M. (1993), "Simplified creep analysis of composite beams with flexible connectors", *J. Struct. Eng.*, **119**(5), 1484-1497. [https://doi.org/10.1061/\(ASCE\)0733-9445\(1993\)119:5\(1484\)](https://doi.org/10.1061/(ASCE)0733-9445(1993)119:5(1484))
- Dezi, L., Leoni, G. and Tarantino, A.M. (1996), "Algebraic methods for creep analysis of continuous composite beams", *J. Struct. Eng. ASCE*, **122**(4), 423-430. [https://doi.org/10.1061/\(ASCE\)0733-9445\(1997\)123:8\(1112\)](https://doi.org/10.1061/(ASCE)0733-9445(1997)123:8(1112))
- Draiche, K., Bousahla, A.A., Tounsi, A., Alwabli, A.S., Tounsi, A. and Mahmoud, S.R. (2019), "Static analysis of laminated reinforced composite plates using a simple first-order shear deformation theory", *Comput. Concrete, Int. J.*, **24**(4), 369-378. <https://doi.org/10.12989/cac.2019.24.4.369>
- Draoui, A., Zidour, M., Tounsi, A. and Adim, B. (2019), "Static and dynamic behavior of nanotubes-reinforced sandwich plates using (FSDT)", *J. Nano Res.*, **57**, 117-135. <https://doi.org/10.4028/www.scientific.net/JNanoR.57.117>
- Guenaneche, B. and Tounsi, A. (2014), "Effect of shear deformation on interfacial stress analysis in plated beams under arbitrary loading", *Adhes. Adhesiv.*, **48**, 1-13. <https://doi.org/10.1016/j.ijadhadh.2013.09.016>
- Gupta, R.K., Kumar, S., Patel, K.A., Chaudhary, S. and Nagpal, A.K. (2015), "Rapid prediction of deflections in multi-span continuous composite bridges using neural networks", *Int. J. Steel Struct.*, **15**(4), 893-909. <https://doi.org/10.1007/s13296-015-1211-9>
- Hadj, B., Rabia, B. and Daouadji, T.H. (2019), "Influence of the distribution shape of porosity on the bending FGM new plate model resting on elastic foundations", *Struct. Eng. Mech., Int. J.*, **72**(1), 823-832. <https://doi.org/10.12989/sem.2019.72.1.061>
- Henriques, D., Gonçalves, R., Sousa, C. and Camotim, D. (2020), "GBT-based time-dependent analysis of

- steel-concrete composite beams including shear lag and concrete cracking effects” , *Thin-Wall. Struct.*, **150**, 106706. <https://doi.org/10.1016/j.tws.2020.106706>
- Jones, R., Swamy, R.N. and Charif, A. (1988), “Plate separation and anchorage of reinforced concrete beams strengthened by epoxy – bonded steel plates”, *Struct. Engr.*, **66**(5/1), 85-94. <http://worldcat.org/issn/14665123>
- Kaddari, M., Kaci, A., Bousahla, A.A., Tounsi, A., Bourada, F., Tounsi, A., Bedia, E.A. and Al-Osta, M.A. (2020), “A study on the structural behaviour of functionally graded porous plates on elastic foundation using a new quasi-3D model: Bending and Free vibration analysis”, *Comput. Concrete, Int. J.*, **25**(1), 37-57. <https://doi.org/10.12989/cac.2020.25.1.037>
- Karami, B., Janghorban, M. and Tounsi, A. (2019a), “Galerkin’s approach for buckling analysis of functionally graded anisotropic nanoplates/different boundary conditions”, *Eng. Comput.*, **35**, 1297-1316. <https://doi.org/10.1007/s00366-018-0664-9>
- Karami, B., Janghorban, M. and Tounsi, A. (2019b), “On pre-stressed functionally graded anisotropic nanoshell in magnetic field”, *J. Brazil. Soc. Mech. Sci. Eng.*, **41**, 495. <https://doi.org/10.1007/s40430-019-1996-0>
- Krou, B., Bernard, F. and Tounsi, A. (2014), “Fibers orientation optimization for concrete beam strengthened with a CFRP bonded plate: A coupled analytical-numerical investigation”, *Eng. Struct.*, **9**, 218-227. <https://doi.org/10.1016/j.engstruct.2013.05.008>
- Kumar, P., Chaudhary, S. and Gupta, R. (2017), “Behaviour of adhesive bonded and mechanically connected steel-concrete composite under impact loading”, *Procedia Eng.*, **173**, 447-454. <https://doi.org/10.1016/j.proeng.2016.12.062>
- Lacki, P., Nawrot, J., Derlatka, A. and Winowiecka, J. (2019), “Numerical and experimental tests of steel-concrete composite beam with the connector made of top-hat profile” , *Compos. Struct.*, **211**, 244-253. <https://doi.org/10.1016/j.compstruct.2018.12.035>
- Larbi, A.S., Ferrier, E., Jurkiewicz, B. and Hamelin, P. (2007), “Static behaviour of steel concrete beam connected by bonding”, *Eng. Struct.*, **29**(6), 1034-1042. <http://dx.doi.org/10.1016/j.engstruct.2006.06.015>
- Liu, S., Zhou, Y., Zheng, Q., Zhou, J., Jin, F. and Fan, H. (2019), “Blast responses of concrete beams reinforced with steel-GFRP composite bars”, *Structures*, **22**, 200-212. <https://doi.org/10.1016/j.istruc.2019.08.010>
- Lowe, D., Roy, K., Das, R., Clifton, C.G. and Lim, J.B. (2020), “Full scale experiments on splitting behaviour of concrete slabs in steel concrete composite beams with shear stud connection”, *Structures*, **23**, 126-138. <https://doi.org/10.1016/j.istruc.2019.10.008>
- Mahmoudi, A., Benyoucef, S., Tounsi, A., Benachour, A., Adda Bedia, E.A. and Mahmoud, S.R. (2019), “A refined quasi-3D shear deformation theory for thermo-mechanical behavior of functionally graded sandwich plates on elastic foundations”, *J. Sandw. Struct. Mater.*, **21**(6), 1906-1926. <https://doi.org/10.1177/1099636217727577>
- Medani, M., Benahmed, A., Zidour, M., Heireche, H., Tounsi, A., Bousahla, A.A., Tounsi, A. and Mahmoud, S.R. (2019), “Static and dynamic behavior of (FG-CNT) reinforced porous sandwich plate using energy principle”, *Steel Compos. Struct., Int. J.*, **32**(5), 595-610. <https://doi.org/10.12989/scs.2019.32.5.595>
- Panjehpour, M., Farzadnia, N., Demirboga, R. and Ali, A.A.A. (2016), “Behavior of high-strength concrete cylinders repaired with CFRP sheets”, *J. Civil Eng. Manag.*, **22**(1), 56-64. <https://doi.org/10.3846/13923730.2014.897965>
- Partov, D. and Kantchev, V. (2007), “Contribution to the methods of analysis of composite steel-concrete beams regarding rheology”, *Eng. Mech.*, **14**(5), 327-343. [http://dlib.lib.cas.cz/5362/1/14\\_5\\_327.pdf](http://dlib.lib.cas.cz/5362/1/14_5_327.pdf)
- Rabahi, A., Daouadji, T.H., Abbes, B. and Adim, B. (2016), “Analytical and numerical solution of the interfacial stress in reinforced-concrete beams reinforced with bonded prestressed composite plate”, *J. Reinf. Plast. Compos.*, **35**(3), 258-272. <https://doi.org/10.1177/0731684415613633>
- Rabia, B., Abderezak, R., Daouadji, T.H., Abbes, B., Belkacem, A. and Abbes, F. (2018), “Analytical analysis of the interfacial shear stress in RC beams strengthened with prestressed exponentially-varying properties plate”, *Adv. Mater. Res., Int. J.*, **7**(1), 29-44. <https://doi.org/10.12989/amr.2018.7.1.029>
- Rabia, B., Daouadji, T.H. and Abderezak, R. (2019), “Effect of distribution shape of the porosity on the

- interfacial stresses of the FGM beam strengthened with FRP plate”, *Earthq. Struct., Int. J.*, **16**(5), 601-609. <https://doi.org/10.12989/eas.2019.16.5.601>
- Rahmani, M.C., Kaci, A., Bousahla, A.A., Bourada, F., Tounsi, A., Bedia, E.A., Mahmoud, S.R., Benrahou, K.H. and Tounsi, A. (2020), “Influence of boundary conditions on the bending and free vibration behavior of FGM sandwich plates using a four-unknown refined integral plate theory”, *Comput. Concrete, Int. J.*, **25**(3), 225-244. <https://doi.org/10.12989/cac.2020.25.3.225>
- Refraci, S., Bousahla, A.A., Bouhadra, A., Menasria, A., Bourada, F., Tounsi, A., Bedia, E.A., Mahmoud, S.R., Benrahou, K.H. and Tounsi, A. (2020), “Effects of hygro-thermo-mechanical conditions on the buckling of FG sandwich plates resting on elastic foundations”, *Comput. Concrete, Int. J.*, **25**(4), 311-325. <https://doi.org/10.12989/cac.2020.25.4.311>
- Sahla, M., Saidi, H., Draiche, K., Bousahla, A.A., Bourada, F. and Tounsi, A. (2019), “Free vibration analysis of angle-ply laminated composite and soft core sandwich plates”, *Steel Compos. Struct., Int. J.*, **33**(5), 663-679. <https://doi.org/10.12989/scs.2019.33.5.663>
- Si, X.T. and Au, F.T. (2011), “An efficient method for time-dependent analysis of composite beams”, *Procedia Eng.*, **14**, 1863-1870. <https://doi.org/10.1016/j.proeng.2011.07.234>
- Smith, S.T. and Teng, J.G. (2002), “Interfacial stresses in plated beams”, *Eng. Struct.*, **23**(7), 857-871. [http://dx.doi.org/10.1016/S0141-0296\(00\)00090-0](http://dx.doi.org/10.1016/S0141-0296(00)00090-0)
- Souici, A., Berthet, J.F., Li, A. and Rahal, N. (2013), “Behaviour of both mechanically connected and bonded steel-concrete composite beams”, *J. Eng. Struct.*, **49**, 11-23. <https://doi.org/10.1016/j.engstruct.2012.10.014>
- Tahar, H.D., Boussad, A., Abderezak, R., Rabia, B., Fazilay, A. and Belkacem, A. (2019), “Flexural behaviour of steel beams reinforced by carbon fibre reinforced polymer: Experimental and numerical study”, *Struct. Eng. Mech., Int. J.*, **72**(4), 409-419. <https://doi.org/10.12989/sem.2019.72.4.409>
- Tounsi, A., Daouadji, T.H. and Benyoucef, S. (2008), “Interfacial stresses in FRP-plated RC beams: Effect of adherend shear deformations”, *Int. J. Adhes. Adhesiv.*, **29**, 343-351. <https://doi.org/10.1016/j.ijadhadh.2008.06.008>
- Tounsi, A., Al-Dulaijan, S.U., Al-Osta, M.A., Chikh, A., Al-Zahrani, M.M., Sharif, A. and Tounsi, A. (2020), “A four variable trigonometric integral plate theory for hygro-thermo-mechanical bending analysis of AFG ceramic-metal plates resting on a two-parameter elastic foundation”, *Steel Compos. Struct., Int. J.*, **34**(4), 511-524. <https://doi.org/10.12989/scs.2020.34.4.511>
- Tsai, M.Y., Oplinger, D.W. and Morton, J. (1998), “Improved theoretical solutions for adhesive lap joints”, *Int. J. Solids Struct.*, **35**(12), 1163-1185. [https://doi.org/10.1016/S0020-7683\(97\)00097-8](https://doi.org/10.1016/S0020-7683(97)00097-8)
- Wang, Y.H., Yu, J., Liu, J.P., Zhou, B.X. and Chen, Y.F. (2020), “Experimental study on assembled monolithic steel-prestressed concrete composite beam in negative moment”, *J. Constr. Steel Res.*, **167**, 105667. <https://doi.org/10.1016/j.jcsr.2019.06.004>
- Zarga, D., Tounsi, A., Bousahla, A.A., Bourada, F. and Mahmoud, S.R. (2019), “Thermomechanical bending study for functionally graded sandwich plates using a simple quasi-3D shear deformation theory”, *Steel Compos. Struct., Int. J.*, **32**(3), 389-410. <https://doi.org/10.12989/scs.2019.32.3.389>
- Zhao, G. and Li, A. (2008), “Numerical study of a bonded steel and concrete composite beam”, *Comput. Struct.*, **86**(19-20), 1830-1838. <https://doi.org/10.1016/j.compstruc.2008.04.002>